NASA
Technical
Paper
3071

March 1991

Compression Behavior of Graphite-Thermoplastic and Graphite-Epoxy Panels With Circular Holes or Impact Damage

Dawn C. Jegley

NASA

NASA Technical Paper 3071

1991

Compression Behavior of Graphite-Thermoplastic and Graphite-Epoxy Panels With Circular Holes or Impact Damage

Dawn C. Jegley
Langley Research Center
Hampton, Virginia

NASA
National Aeronautics and Space Administration
Office of Management
Scientific and Technical Information Division

The use of trademarks or names of manufacturers in this report is for accurate reporting and does not constitute an official endorsement, either expressed or implied, of such products or manufacturers by the National Aeronautics and Space Administration.

Summary

An experimental investigation of the compression behavior of laminated specimens made from graphite-epoxy tape (AS4-3502), graphite-thermoplastic tape (AS4-PEEK), and graphite-thermoplastic fabric (AS4-PEEK) was conducted. Specimens with five different stacking sequences were loaded to failure in uniaxial compression. Some of the specimens had central circular holes with diameters up to 67 percent of the specimen width. Other specimens were subjected to low-speed impact with impact energies up to 35 J prior to compressive loading. This investigation indicates that graphite-thermoplastic specimens with holes have up to 15 percent lower failure stresses and strains than graphite-epoxy specimens with the same stacking sequence and hole size. However, graphite-thermoplastic specimens subjected to low-speed impact have up to 15 percent higher failure stresses and strains than graphite-epoxy specimens with the same stacking sequence and impact energy. Compression tests of graphite-thermoplastic specimens constructed of fabric and unidirectional tape indicate that the material form has little effect on failure strains in specimens with holes or low-speed impact damage.

Introduction

Lightweight composite materials are increasingly being used in aircraft structures. The structural response of laminated composites containing thermoplastic resin must be evaluated before they can be considered for application to civil transport aircraft structures. Quasi-isotropic graphite-thermoplastic laminates have been evaluated (e.g., ref. 1), but other stacking sequences should be considered since all laminates do not exhibit the same behavior. An experimental investigation of the compression behavior of laminated specimens made from graphite-epoxy tape (AS4-3502), graphite-thermoplastic tape (AS4-PEEK), and graphite-thermoplastic fabric (AS4-PEEK) has been conducted, and the results of the investigation are presented in the present paper. Results for specimens in two categories are presented: specimens with 0° plies and specimens with no 0° plies. Specimens with thicknesses ranging from 0.11 to 0.46 cm were constructed and loaded to failure in uniaxial compression. Some specimens had central circular holes with diameters up to 65 percent of the specimen width. Other specimens were subjected to low-speed impact with impact energies up to 35 J and then loaded to failure in uniaxial compression.

Test Specimens

The graphite-epoxy specimens tested in this investigation were fabricated from commercially available Hercules AS4 graphite fiber and 3502 thermosetting epoxy resin. Graphite-epoxy specimens were made from unidirectional tape and are designated with the letter E in table I. The graphite-thermoplastic specimens were fabricated from commercially available Hercules AS4 graphite fiber and ICI PEEK resin. Graphite-thermoplastic specimens made from unidirectional tape are designated with the letter T in table I. Graphite-thermoplastic specimens in which the ±45° plies were made from woven fabric are designated with the letter F in table I. The five stacking sequences considered are as follows:

Stacking sequence 1
$[(\pm 45)_2/0_4/90/\pm 45/0_2/90]_s$

Stacking sequence 2
$[(\pm 45)_3/0_2/90/(\pm 45)_2/0/\overline{90}]_s$

Stacking sequence 3
$[\pm 45/0_6/\pm 45/0_6]_s$

Stacking sequence 4
$[\pm 45/0_6/\pm 45/0_6/\overline{90}]_s$

Stacking sequence 5
$[(\pm 45)_2/\overline{90}]_s$

Each specimen type is designated by a letter indicating the material and a number indicating the stacking sequence. Individual specimens are identified by a specimen type followed by a number from 1 through 15. For example, the first specimen tested was made from graphite-thermoplastic tape with stacking sequence $[(\pm 45)_2/0_4/90/\pm 45/0_2/90]_s$ and is designated T1-1. The stacking sequences, specimen designations, and the number of specimens tested of each type are listed in table I. All specimens were nominally 25.4 cm long and either 7.62 or 10.16 cm wide. Centrally located circular holes were machined into some of the specimens with diamond-impregnated-core drills. Specimen cross-sectional area and hole size are listed in tables II and III. Nominal material properties of both material systems are listed in table IV. The loaded ends of each specimen were machined flat and parallel to permit uniform end displacement. All specimens were ultrasonically C-scanned to establish specimen quality prior to testing.

Apparatus and Tests

Test specimens were loaded in uniaxial compression using a hydraulic testing machine. The loaded ends of the specimen were clamped by fixtures during testing, and the sides were simply supported by restraints to prevent the specimen from buckling as a wide column. A typical specimen mounted in the support fixture is shown in figure 1(a). Electrical resistance strain gages were used to monitor strains,

and dc differential transformers were used to monitor displacements. The locations of the back-to-back strain gages used to monitor the far-field laminate strains in all specimens and along a horizontal line between the edge of the hole and the side of the specimen are shown in figure 1. All specimens were painted white on one side to give a reflective surface so that a moiré fringe technique could be used to monitor out-of-plane deformation patterns.

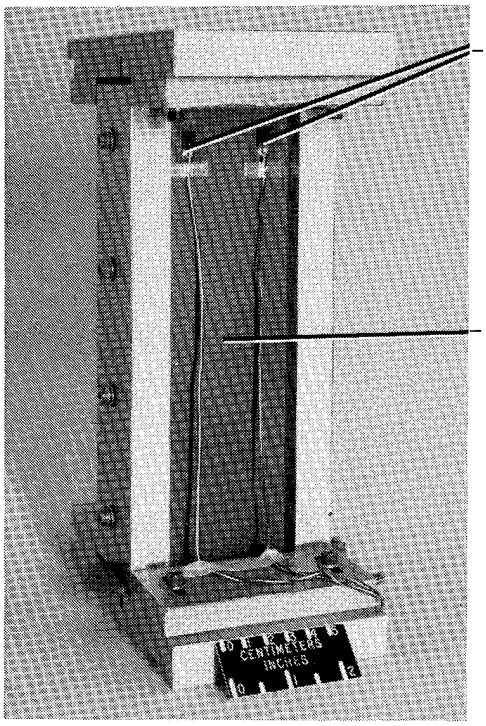

(a) Typical specimen in test fixture.

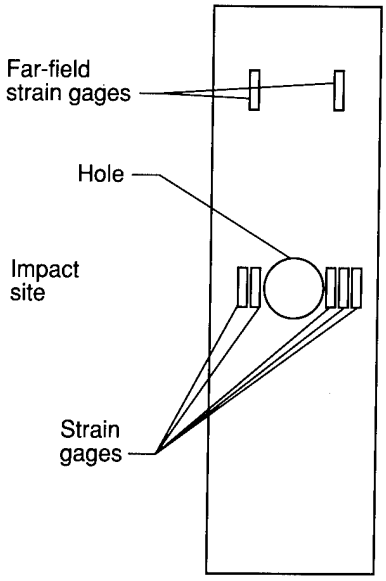

(b) Strain gage pattern for a typical specimen with a hole.

Figure 1. Specimen configuration.

A procedure detailed in reference 2 was used in the current study for impacting specimens. Aluminum spheres 1.27 cm in diameter were used as impact projectiles. The projectiles were directed normal to the plane of the specimen at speeds from 15 to 153 m/sec corresponding to impact energies from 0.35 to 35 J. All specimens were impacted at the center of the test section. The applied load, the displacement of the loading platen, and the strain gage signals were recorded at regular intervals.

Results and Discussion

Test results for specimens constructed with five stacking sequences (listed in table I) are presented in this section. A comparison is made between specimens with the same stacking sequence constructed from graphite-epoxy tape and graphite-thermoplastic tape, specimens with the same stacking sequence constructed from graphite-thermoplastic tape and fabric, and specimens constructed from graphite-thermoplastic tape or graphite-epoxy tape with clustered 0° plies and separated 0° plies. Specimen stiffness, strain concentrations around holes, and the effects of holes or impact damage on failure strain are discussed. Postbuckling of thin specimens is also discussed.

Control Specimens

Control specimens (those without holes or impact damage) were constructed with each stacking sequence studied. Control specimens made from graphite-epoxy and graphite-thermoplastic materials with stacking sequence $[(\pm 45)_2/0_4/90/\pm 45/0_2/90]_s$, designated E1-1 and T1-1, respectively, in table II, buckled prior to failure. Moiré fringe patterns indicate that control specimen E1-1 buckled into three half-waves while control specimen T1-1 buckled into one half-wave at about 70 percent of the failure load. The stress-strain relationships for these control specimens are shown in figure 2. The slope of these curves indicates that the prebuckling stiffness of specimen E1-1 (which is 5 percent thicker than specimen T1-1) is about 8 percent higher than the prebuckling stiffness of specimen T1-1 even though they have the same stacking sequence. A change in slope (stiffness) in the stress versus strain curve indicates the onset of buckling. A slight reduction in stiffness at buckling can be seen in figure 2 at a stress of about 400 MPa. Both control specimens E1-1 and T1-1 failed near a clamped edge.

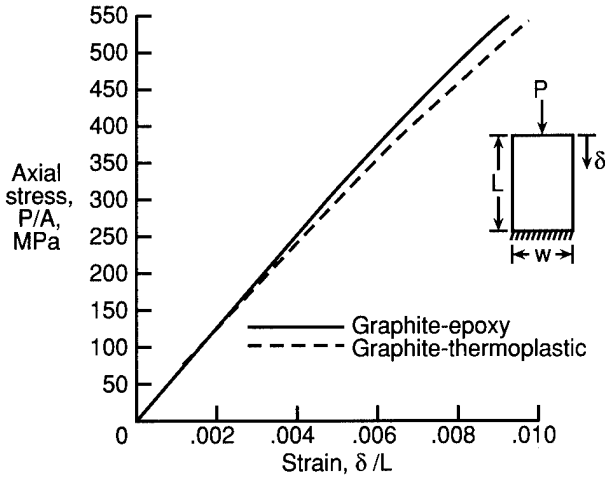

Figure 2. Compression stress-strain behavior for control specimens E1-1 and T1-1 with stacking sequence $[(\pm 45)_2/0_4/90/\pm 45/0_2/90]_s$. A is cross-sectional area.

Control specimens with stacking sequence $[(\pm 45)_3/0_2/90/(\pm 45)_2/0/\overline{90}]_s$ made from graphite-thermoplastic tape and woven fabric, designated T2-1 and F2-1, respectively, buckled into three half-waves immediately prior to failure near a clamped edge. The stress-strain relationships for control specimens of types T2 and F2 are shown in figure 3. Since these specimens contain 69 percent ±45° plies, their stress-strain relationships are nonlinear, indicating nonlinear material properties. The slope of the curves indicates that the difference in prebuckling stiffness of the two specimens is approximately the same. The fabric specimen failed at a higher stress and strain than the tape specimen.

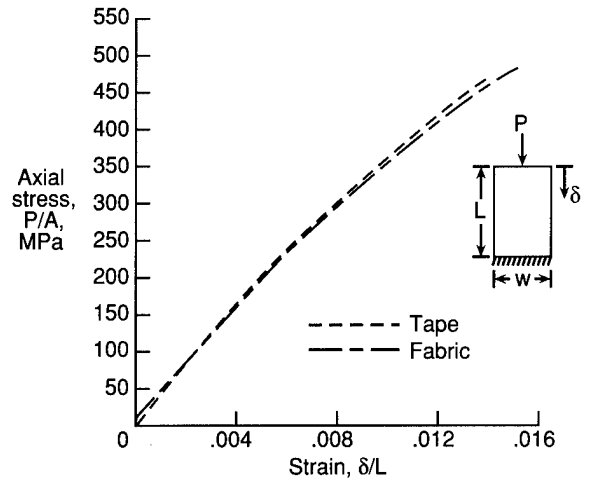

Figure 3. Compression stress-strain behavior for control specimens T2-1 and F2-1 with stacking sequence $[(\pm 45)_3/0_2/90/(\pm 45)_2/0/\overline{90}]_s$. A is cross-sectional area.

In graphite-epoxy specimens, conventional stacking sequences rarely contain many plies of the same orientation clustered together. To determine whether clustering many 0° plies in the center of a graphite-thermoplastic laminate influences failure due to uniaxial compressive loading, two stacking sequences were studied. Control specimens made from graphite-thermoplastic tape with stacking sequences $[\pm 45/0_6/\pm 45/0_6]_s$ and $[\pm 45/0_6/\pm 45/0_6/\overline{90}]_s$, designated T3-1 and T4-1, respectively, did not buckle prior to failure. Both control specimens T3-1 and T4-1 failed near a clamped edge at approximately the same failure strain. The damage in the failed specimen was confined to a region within about 3 cm of the clamping fixture. Specimen T4-1 is about 5 percent thicker and stiffer than specimen T3-1. Control specimens made from graphite-epoxy tape with the same two stacking sequences, designated E3-1 and E4-1, buckled prior to failure and failed near a clamped edge. The failure of specimen E3-1 involved delamination of the outer two plies over approximately one third of the specimen. Interior delaminations were apparent in approximately half of the specimen. Specimen E4-1 failed in the same way as specimen T4-1. Failure strains for these four control specimens differ by less than 5 percent.

All previously mentioned specimens contain 28 or more plies. These relatively thick specimens display a different behavior than specimens containing significantly fewer plies. To compare relatively thin specimens, graphite-epoxy tape, graphite-thermoplastic tape, and graphite-thermoplastic fabric specimens (designated as specimen types E5, T5, and F5, respectively) with stacking sequence $[(\pm 45)_2/\overline{90}]_s$ were studied. The stress-strain relationships for the control specimens of specimen types E5, T5, and F5 are shown in figure 4. The fabric specimen is about 12 percent thinner and about 10 percent less stiff than the tape specimens. The control specimens of specimen types E5, T5, and F5 buckled into four half-waves of approximately equal wavelength then failed at midlength of the specimen (along a nodal line). Each specimen carried load well into the postbuckling range. Failure strain for the graphite-epoxy control specimen was 35 percent and 20 percent lower than the failure strain for the graphite-thermoplastic fabric and tape specimens, respectively. The graphite-thermoplastic fabric specimen had the highest failure strain, 0.0138. The change in stiffness in the stress-strain curve indicates that buckling occurred in all three specimens at a stress of approximately 75 MPa. The prebuckling stiffness in the graphite-epoxy specimen is about 10 percent higher than the prebuckling stiffness in the graphite-thermoplastic specimens. The postbuckling stiffness in the graphite-epoxy specimen is about 25 percent higher than the postbuckling

stiffness in the graphite-thermoplastic specimens. The shear stiffness of a graphite-thermoplastic 0° lamina is 15 percent lower than the shear stiffness of a graphite-epoxy 0° lamina. Since this $[(\pm 45)_2/\overline{90}]_s$ laminate is 88 percent ±45° plies, the graphite-thermoplastic specimens have lower laminate stiffnesses.

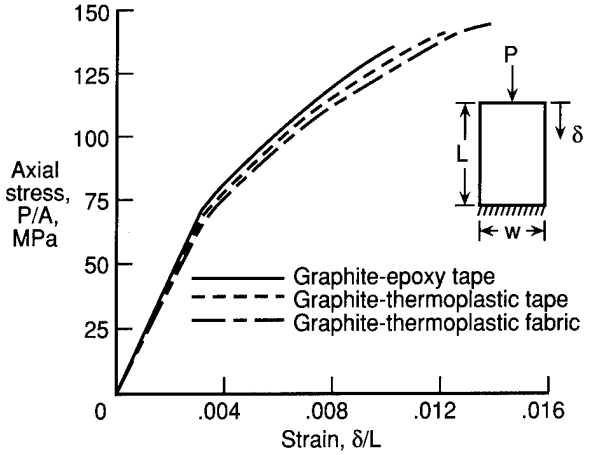

Figure 4. Compression stress-strain behavior for control specimens of types E5, T5, and F5 with stacking sequence $[(\pm 45)_2/\overline{90}]_s$. A is cross-sectional area.

Specimens With 0° Plies

Specimens With Holes

Strain distributions around holes. An analysis was conducted using the finite-element code EAL (ref. 3) to examine strain distributions around a hole for specimens of types E1 and T1. In the finite-element analysis one quarter of the specimen was modeled. The finite-element grids contained approximately 175 quadrilateral elements. The elements used near the hole edge were smaller than those away from the hole. Specific grid configurations varied from one hole size to the next. Typical properties of AS4-3502 are shown in table IV. Properties of AS4-PEEK presented in the literature (refs. 4–6) vary somewhat. The properties shown in table IV were used in this study.

Normalized strain distributions based on strain gage measurements and analytical predictions for specimens with hole diameters of 0.794 and 2.54 cm are shown in figure 5. For the specimens with the larger hole, the strains predicted for the graphite-thermoplastic specimens are slightly higher than those predicted for the graphite-epoxy specimens. This trend is not apparent in the experimental results. No difference between the strain distributions of the two material systems can be seen for the specimens with the smaller hole. A study of strain distributions around holes presented in reference 7 indicates that the difference in strain concentration at the edge of the hole is a finite-width effect, i.e., dependent upon a/w, where a is the hole diameter and w is the plate width. The strain concentration is higher for the graphite-thermoplastic specimen than for the graphite-epoxy specimen for the larger hole size shown, indicating that the graphite-thermoplastic specimens are more notch sensitive (ref. 7) than the graphite-epoxy specimens.

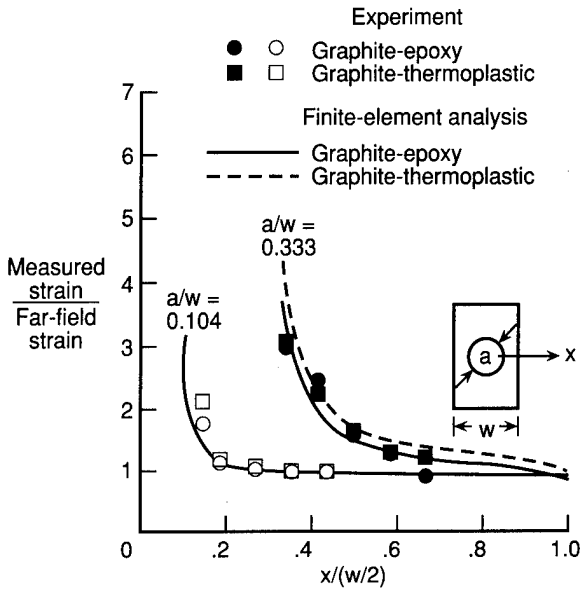

Figure 5. Longitudinal strain distribution at hole for specimens with stacking sequence $[(\pm 45)_2/0_4/90/\pm 45/0_2/90]_s$.

Failure characteristics. The effect of hole size on failure strain is shown in figure 6(a) for graphite-epoxy and graphite-thermoplastic specimens with stacking sequence $[(\pm 45)_2/0_4/90/\pm 45/0_2/90]_s$ (specimens of types E1 and T1). Specimen geometry, failure stress, and failure strain are shown in table II for all specimens of types E1 and T1 tested.

All specimens of types E1 and T1 with holes failed through the hole and exhibited no buckling behavior. Failure strain is 5 to 30 percent higher for specimens of type E1 than for specimens of type T1 with the same hole size. Failure of each specimen involved delamination between plies and laminate failure in transverse cracking across the specimen, as shown in the photographs of specimens E1-7 and T1-5 in figure 6(b). Failed fibers became wedged between other fibers during failure. The failure of the graphite-thermoplastic specimens at consistently lower stresses and strains than the graphite-epoxy specimens may be related to the lower shear stiffness of the AS4-PEEK material. However, since this $[\pm 45_2/0_4/90/\pm 45/0_2/90]_s$ laminate contains only 43 percent ±45° plies, matrix shearing is

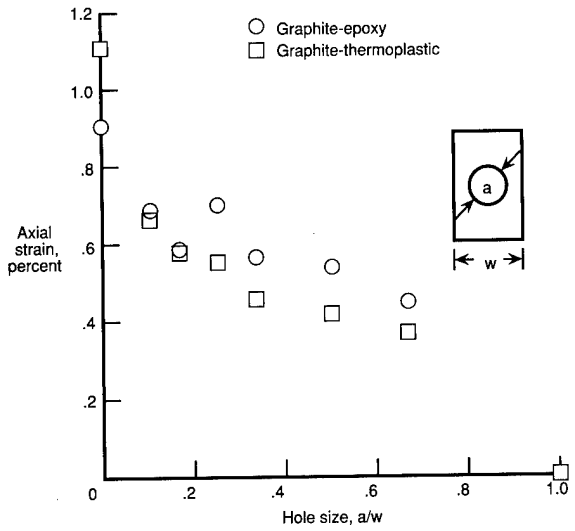

(a) Failure strain as a function of hole size.

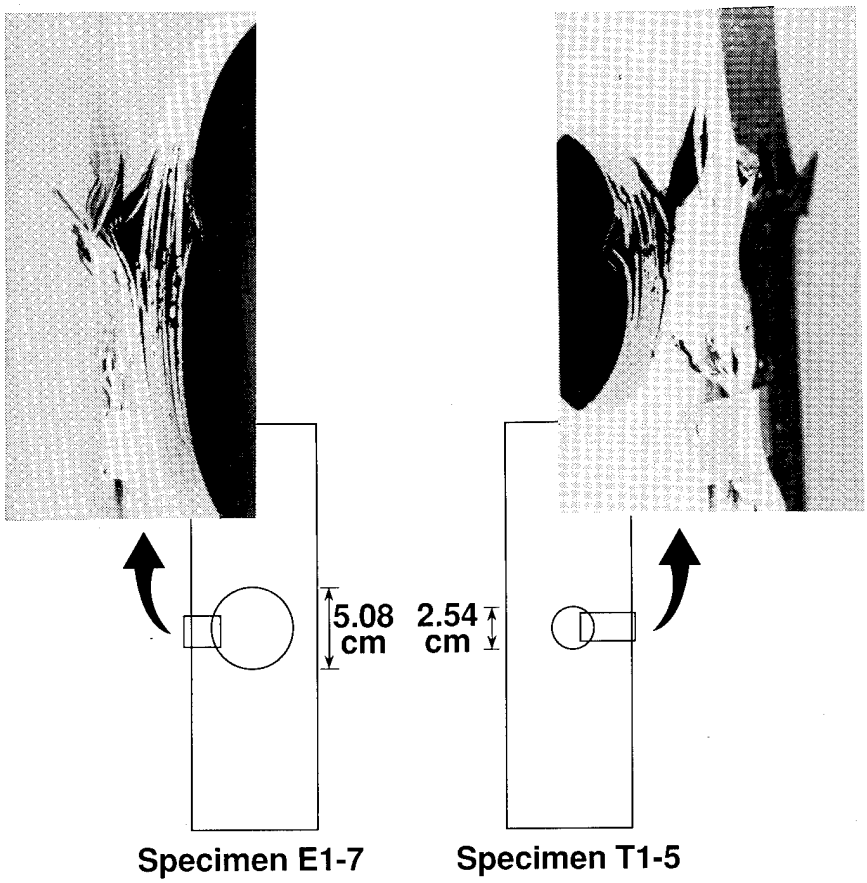

L-91-01

(b) Failure mode.

Figure 6. Results for specimens with stacking sequence $[(\pm 45)_2/0_4/90/\pm 45/0_2/90]_s$.

not the dominant failure mode. No matrix shearing bands (ref. 8) are evident after failure. C-scans of specimens after testing indicate that off-axis (in the $\pm 45°$ directions) and longitudinal (in the 0° direction) cracking occurred during loading in both the graphite-epoxy and the graphite-thermoplastic specimens. The graphite-thermoplastic specimens behaved similar to the graphite-epoxy specimens with small hole sizes ($a/w < 0.25$), but the graphite-epoxy specimens failed at significantly higher strains than the graphite-thermoplastic specimens when larger holes were present.

The effect of hole size on failure strain is shown in figure 7 for specimens with stacking sequence $[(\pm 45)_3/0_2/90/(\pm 45)_2/0/\overline{90}]_s$ made from graphite-thermoplastic tape and graphite-thermoplastic woven fabric, designated as specimen types T2 and F2, respectively. Average specimen cross-sectional area away from the hole and the range of hole sizes considered are presented in table III. All specimens of types T2 and F2 with holes failed through the hole and exhibited no buckling behavior. Failure strains are almost identical for specimens of the same hole size for the two material forms, as shown in figure 7. C-scans made of specimens after failure indicate that no off-axis cracking occurred in any of the specimens of type T2 or F2. Some longitudinal cracking occurred in the specimens with large holes.

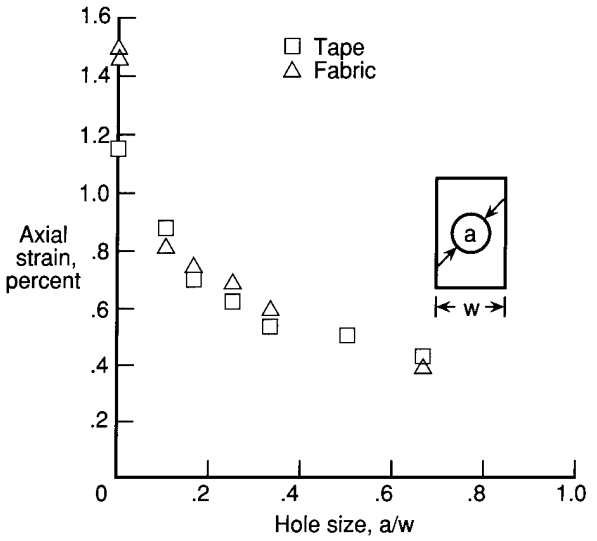

Figure 7. Failure strain as a function of hole size for graphite-thermoplastic specimens with stacking sequence $[(\pm 45)_3/0_2/90/(\pm 45)_2/0/\overline{90}]_s$.

To determine whether clustering many 0° plies in the center of a graphite-thermoplastic laminate influences the failure of specimens with holes, graphite-thermoplastic specimens made from tape with stacking sequences $[\pm 45/0_6/\pm 45/0_6]_s$ and $[\pm 45/0_6/\pm 45/0_6/\overline{90}]_s$, designated as specimen types T3 and T4, respectively, were examined. Graphite-epoxy specimens with the same two stacking sequences, designated E3 and E4, were also tested. The average far-field cross-sectional area of these specimens and the range of hole sizes considered are presented in table III. The effect of hole size on failure strain is shown in figure 8(a) for these specimens. A comparison of the failure strains of the specimens indicates that there is no consistent difference in the results for the two stacking sequences. The clustered 0° plies do not induce premature failure in the graphite-thermoplastic specimens with holes. However, there is a significant difference in the failure strains for the graphite-epoxy specimens of the two stacking sequences with holes. Specimens of type E3 carried up to 26 percent more strain before failure than specimens of type E4. The clustering of 0° plies does influence the failure strain and does cause premature failure in the graphite-epoxy specimens with holes.

No specimens of type T3 or T4 buckled prior to failure, but specimens of types E3 and E4 with $a/w = 0.104$ did buckle before failure. All specimens with holes failed through the hole. A photograph of the edge of the hole in specimen T4-6 with a 5.08-cm-diameter hole is shown in figure 8(b). Delamination between 0° and +45° or −45° plies is the primary cause of failure in graphite-thermoplastic and graphite-epoxy specimens with these stacking sequences. Delamination can be seen at the edge of the hole. Transverse cracks formed across the width of the specimen, starting at the points on the edge of the hole closest to the unloaded edges in specimens of types T3 and T4. However, specimens of types E3 and E4 exhibited a different failure mode. Specimens of types E3 and E4 with holes of geometry $a/w = 0.333$ exhibited stress concentrations and initial failures at points on the hole edge 45° away from the longitudinal centerline, as shown by the moiré fringe pattern of specimen E4-3 at 86 percent of the failure load (fig. 8(c)). The 90° ply in the center of the graphite-epoxy specimen prevents the specimen from delaminating in the way the graphite-epoxy specimen with the clustered 0° plies does and, therefore, the failure strain is higher and a different failure mechanism results. C-scans of failed specimens indicate that graphite-epoxy specimens exhibited longitudinal cracking while graphite-thermoplastic specimens did not.

Specimens With Impact Damage

The effect of impact damage on failure strain is shown in figure 9 for specimens with stacking sequence $[(\pm 45)_2/0_4/90/\pm 45/0_2/90]_s$ made from graphite-epoxy tape and graphite-thermoplastic tape,

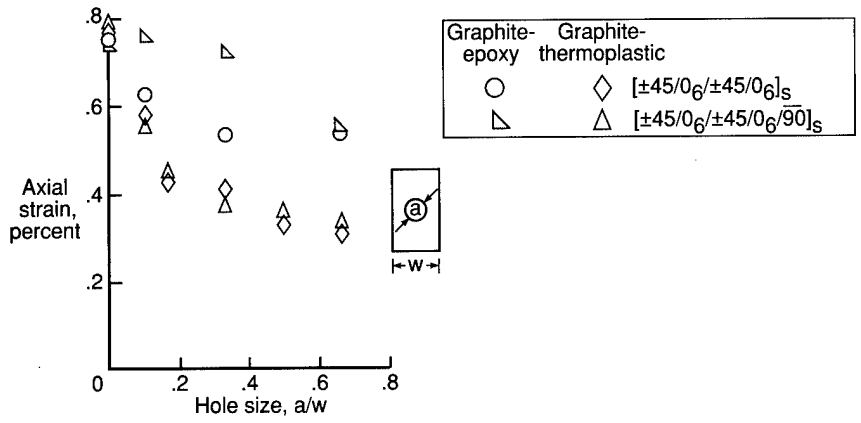

(a) Failure strain as a function of hole size.

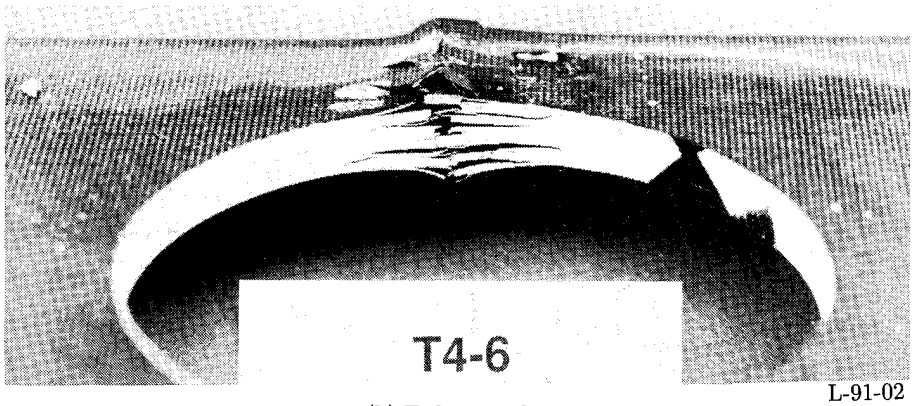

(b) Failure mode.

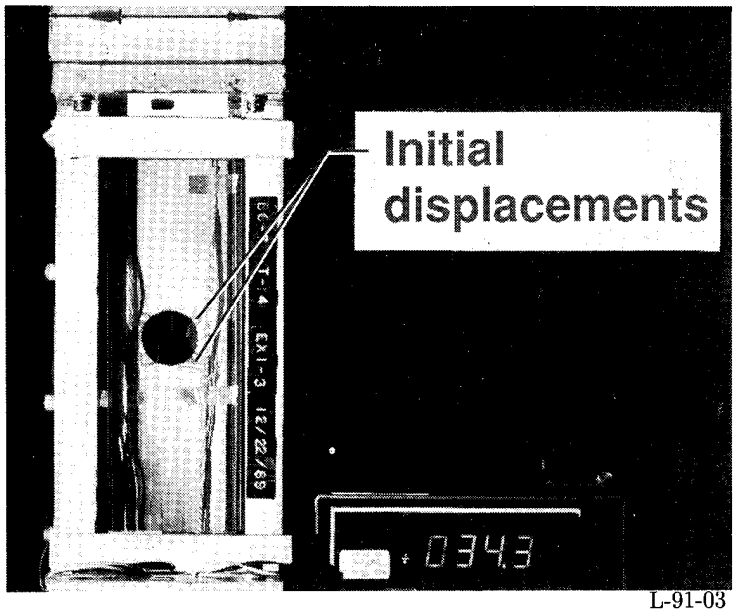

(c) Moiré pattern showing deformation of specimen E4-3 at 86 percent of failure load.

Figure 8. Results for graphite-thermoplastic and graphite-epoxy specimens with stacking sequences $[\pm 45/0_6/\pm 45/0_6]_s$ and $[\pm 45/0_6/\pm 45/0_6/\overline{90}]_s$.

designated as specimen types E1 and T1, respectively. Specimen cross-sectional area, impact energy, failure stress, and failure strain are presented in table II for all specimens of types E1 and T1 tested. Graphite-epoxy specimens not impacted or impacted at about 30 m/sec (1.4 J of impact energy), specimens E1-1 and E1-8 in table II, buckled into three half-waves and failed at an end of the specimen.

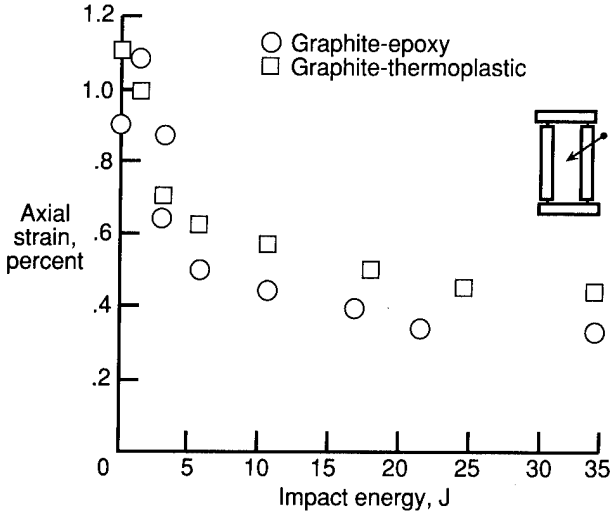

Figure 9. Failure strain as a function of impact energy for specimens with stacking sequence $[(\pm 45)_2/0_4/90/\pm 45/0_2/90]_s$.

Graphite-thermoplastic specimens not impacted or impacted at about 30 m/sec, specimens T1-1 and T1-8 in table II, buckled into one half-wave and failed at an end of the specimen. Specimen E1-9 (3.17 J of impact energy) also buckled into three half-waves but failed through the impact site. No other specimens buckled. All other specimens failed through the impact site. Failure loads for specimens with end failures were about the same, independent of material or impact damage. Specimens subjected to impact speeds greater than 31 m/sec show significant reduction in load-carrying ability due to impact damage in both materials; however, this reduction is more pronounced in the graphite-epoxy specimens. For impact speeds greater than 92 m/sec (12.5 J of impact energy), failure strain remains constant as impact speed increases. C-scans made of specimens after impact but before compressive loading reveal that for impact speeds less than 92 m/sec, the graphite-epoxy specimens have more damage than the graphite-thermoplastic specimens for each impact speed. However, for impact speeds greater than 92 m/sec, the graphite-thermoplastic specimens sustained more damage than the graphite-epoxy specimens. C-scans made for specimens subjected to all impact speeds indicate that damage is confined to an oval around the impact site. There is no longitudinal splitting or off-axis damage propagation for either type of material. The graphite-epoxy and graphite-thermoplastic specimens subjected to severe impact damage (impact speeds greater than 92 m/sec) failed at about 33 percent and 45 percent, respectively, of the failure strain of the undamaged specimens. The failure mode in impacted specimens that did not buckle, as in the specimens with holes, involved delaminations. The same failure mode (dominated by delamination) as described in reference 9 for quasi-isotropic graphite-epoxy specimens subjected to impact damage is seen in specimens of both material systems in this study.

The effect of impact damage on failure strain is shown in figure 10 for graphite-thermoplastic specimens with stacking sequence $[(\pm 45)_3/0_2/90/(\pm 45)_2/0/\overline{90}]_s$ made from tape (specimens of type T2) and from woven fabric (specimens of type F2). The range of impact energies is presented in table III. All specimens subjected to impact speeds of 31 to 46 m/sec (impact energies of 1.4 to 3.3 J) buckled prior to failure. Specimens subjected to higher impact speeds did not buckle. Specimens impacted at 31 m/sec failed at one end of the specimen. The tape specimen impacted at 47 m/sec buckled into three half-waves then failed at a nodal line, away from the impact site. All other impact-damaged specimens failed at the impact site. The mode of failure in all specimens involved delamination and fiber breakage. The tape specimens exhibited more delamination than the fabric specimens because in the fabric specimens each pair of $\pm 45°$ plies is woven together and cannot delaminate. Failure strains are almost the same for tape and fabric specimens, as shown in figure 10.

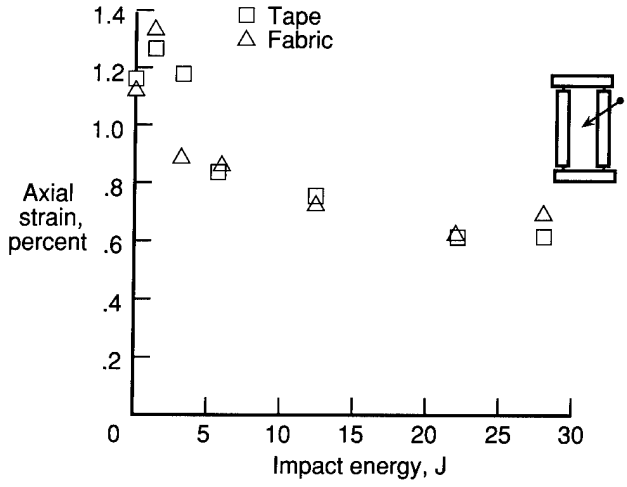

Figure 10. Failure strain as a function of impact energy for graphite-thermoplastic specimens with stacking sequence $[(\pm 45)_3/0_2/90/(\pm 45)_2/0/\overline{90}]_s$.

To determine whether clustering many 0° plies in the center of a graphite-thermoplastic or a graphite-epoxy laminate influences the failure of specimens subjected to low-speed impact, graphite-thermoplastic and graphite-epoxy specimens made from tape with stacking sequences $[\pm 45/0_6/\pm 45/0_6]_s$ (specimen types T3 and E3) and $[\pm 45/0_6/\pm 45/0_6/\overline{90}]_s$ (specimen types T4 and E4) are examined. The range of impact energies considered is listed in table III. No specimens of type T3 or T4 buckled prior to failure. Those impacted with energies less than 1 J failed near a clamped edge. Specimens of types E3 and E4 impacted with energies less than 3 J buckled prior to failing near a clamped edge. All other impacted specimens failed through the impact site. Delamination was the primary cause of failure. Transverse cracks formed across the specimen as the matrix failed. Despite the high percentage of 0° plies (75 percent), C-scans made after severe impact and compressive loading reveal no indication of longitudinal cracks as are described in reference 9 for failures of unidirectional laminates in graphite-thermoplastic specimens; however, longitudinal cracks are evident in the graphite-epoxy specimens. The effect of impact damage on failure strain is shown in figure 11 for the specimens of types T3, T4, E3, and E4.

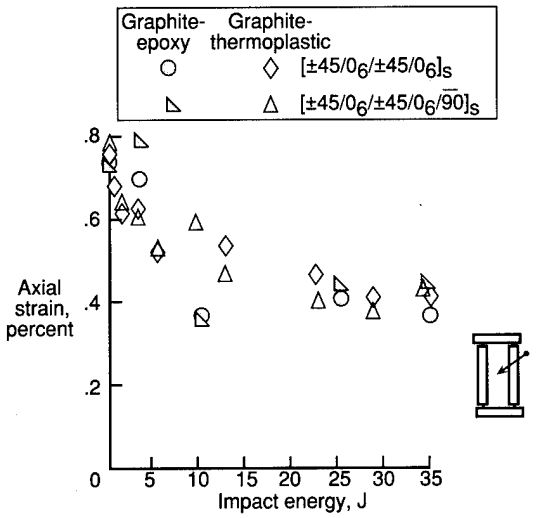

Figure 11. Failure strain as a function of impact energy for graphite-epoxy and graphite-thermoplastic specimens with stacking sequences $[\pm 45/0_6/\pm 45/0_6]_s$ and $[\pm 45/0_6/\pm 45/0_6/\overline{90}]_s$.

There is no consistent difference between the failure strains of graphite-thermoplastic specimens of the two stacking sequences. The clustered 0° plies do not induce premature failure in graphite-thermoplastic specimens subjected to impact damage. Specimens of type E4 have slightly higher failure strains than specimens of type E3 but not a significant enough increase to clearly indicate that the clustering of 0° plies induces premature failure in graphite-epoxy specimens subjected to impact damage.

Specimens With No 0° Plies

Specimens With Holes

Strain distributions around holes. Normalized prebuckling strain distributions based on strain gage measurements and analytical predictions for specimens with hole diameters of 0.794, 2.54, and 3.81 cm are shown in figure 12. These distributions indicate that the graphite-thermoplastic tape specimens have the highest ratio of local strain to far-field strain and that the graphite-thermoplastic fabric specimens have the lowest ratio for all hole sizes. Material properties for fabric specimens are assumed to be the same as for tape specimens made of graphite-thermoplastic material, but the thickness of the specimens differs by about 7 percent. The calculated strain ratios are the same for the graphite-thermoplastic fabric and tape specimens.

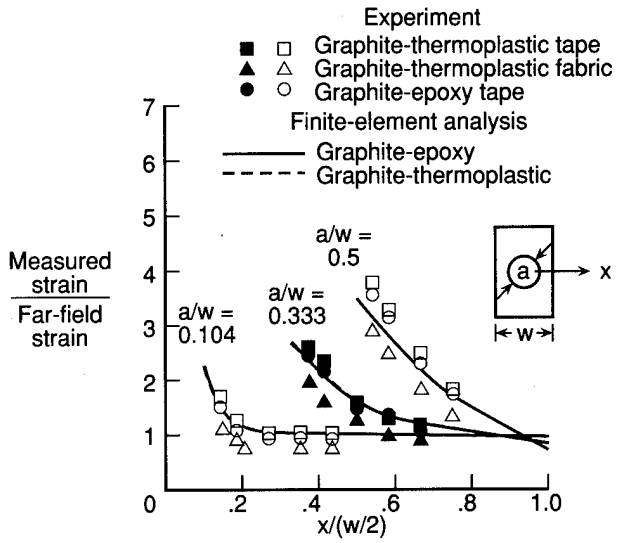

Figure 12. Longitudinal strain distribution at hole for specimens with stacking sequence $[(\pm 45)_2/\overline{90}]_s$.

Failure characteristics. The prebuckling stiffness of a finite-width specimen may be affected by the size of a hole. The prebuckling stiffness of specimens with large holes is not the same as the prebuckling stiffness of control specimens or specimens with small holes. This difference in prebuckling stiffness for graphite-epoxy tape specimens with stacking sequence $[(\pm 45)_2/\overline{90}]_s$ is shown in figure 13. Specimens of this type with large holes buckle at much lower loads than specimens with smaller holes. This reduction in prebuckling stiffness and in buckling load is caused by a combination of the effect of the large hole

and the significant anisotropic effects inherent in this stacking sequence. For this laminate, the ratios of the anisotropic terms to the longitudinal bending stiffness, D_{16}/D_{11} and D_{26}/D_{11}, are approximately 0.25. All three types of specimens demonstrate a similar reduction in prebuckling stiffness as hole size increases for this stacking sequence.

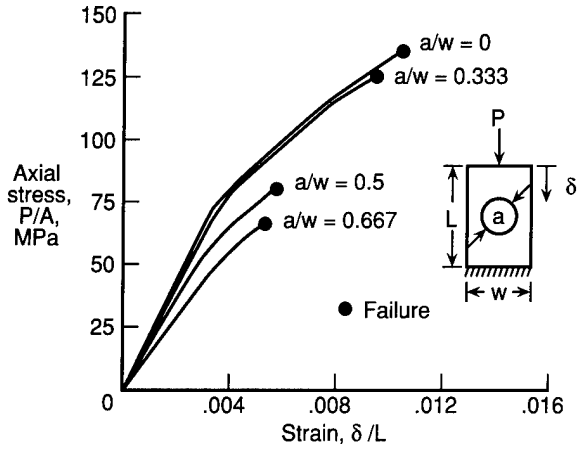

Figure 13. Change in stiffness of graphite-epoxy specimen with stacking sequence $[(\pm 45)_2/\overline{90}]_s$ as hole size changes. A is cross-sectional area.

The effects of hole size on failure stress are shown in figure 14 for specimens with stacking sequence $[(\pm 45)_2/\overline{90}]_s$ made from graphite-epoxy tape (specimen type E5), graphite-thermoplastic tape (specimen type T5), and graphite-thermoplastic fabric (specimen type F5). The range of hole sizes considered is presented in table III for all specimens of types E5, T5, and F5 tested. The specimens of types E5, T5, and F5 with holes buckled into three or more half-waves (often with different wavelengths) with one half-wave centered around the hole. Buckling became evident in moiré patterns at or below 40 percent of the failure load of the undamaged specimen in specimens with small holes. Buckling became evident in moiré patterns at less than 20 percent of the failure load of the undamaged specimen for specimens with large holes. The failure mode of all specimens involved delamination and transverse cracking. C-scans made after testing indicate that no longitudinal or off-axis cracking occurred in the graphite-thermoplastic specimens, but both types of cracks appeared in the graphite-epoxy specimens. The specimens with smaller holes failed at a nodal line in the top half of the specimen. Holes with $a/w < 0.4$ have almost no effect on failure stress for all three types of specimens. The graphite-epoxy specimens with $a/w < 0.4$ have 20 percent lower failure stresses than the graphite-thermoplastic specimens. The specimens with larger holes ($a/w > 0.4$) fail through the hole. Failure stresses for graphite-epoxy specimens with larger holes are slightly lower than those for the graphite-thermoplastic specimens. The graphite-thermoplastic fabric specimens can withstand 10–20 percent higher stress than the graphite-epoxy specimens. The failure stresses of the graphite-thermoplastic tape specimens are 5–10 percent above those of the graphite-epoxy specimens.

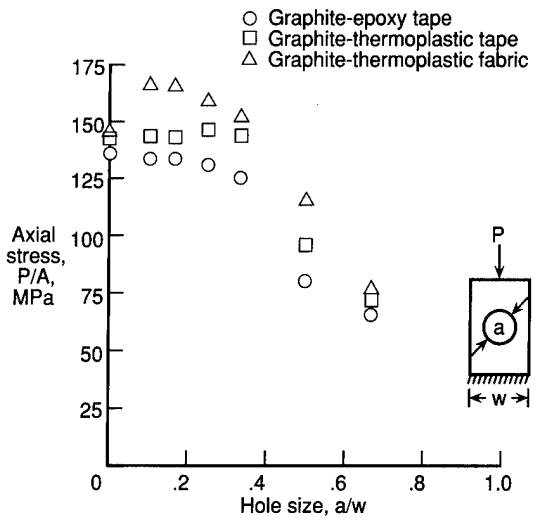

Figure 14. Failure strain as a function of hole size for specimens with stacking sequence $[(\pm 45)_2/\overline{90}]_s$. A is cross-sectional area.

Specimens With Impact Damage

The effects of impact damage on failure stress are shown in figure 15 for specimens with stacking sequence $[(\pm 45)_2/\overline{90}]_s$ made from graphite-epoxy tape (specimen type E5), graphite-thermoplastic tape (specimen type T5), and graphite-thermoplastic fabric (specimen type F5). The range of impact energies considered is presented in table III for all specimens of types E5, T5, and F5 tested.

All impacted specimens buckled prior to failure. Specimens subjected to low impact energies (less than 5.5 J with impact speeds less than about 61 m/sec) failed the same way that the control specimens failed. The specimens buckled into four half-waves with a nodal line through the impact site. The specimens failed at this nodal line by transverse cracking across the width of the specimen. Similar results are presented in reference 10 for specimens with thicknesses ranging from 0.20 to 0.33 cm and impacted at speeds up to 95 m/sec.

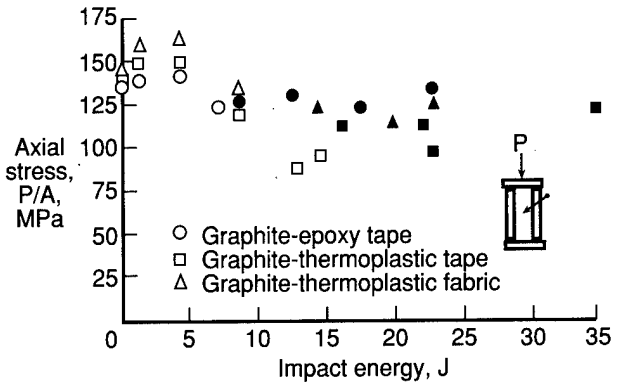

Figure 15. Failure strain as a function of impact energy for specimens with stacking sequence $[(\pm 45)_2/\overline{90}]_s$ (open symbols represent cases when the impact projectile did not fully penetrate the specimen, filled symbols represent cases when the impact projectile did). A is cross-sectional area.

Specimens subjected to impact energies greater than 6 J buckled into three, four, or five half-waves with one half-wave centered on the impact site, and the specimens failed through the impact site by transverse cracking. The wavelengths of each half-wave within a specimen were not necessarily the same. Off-axis cracking is evident in the specimens after impact and before compressive loading for all specimens with impact speeds more than about 61 m/sec (impact energy of 5.5 J). All impact specimens failed through the center of the specimen (impact site) except the fabric specimen impacted at 107 m/sec (impact energy of 17 J), which buckled into two half-waves then failed near the center of one of the half-waves. C-scans made after the test of this specimen indicate that no longitudinal or off-axis cracking occurred. All three types of specimens have approximately the same failure stress for impact speeds less than about 61 m/sec. Above 61 m/sec, all three types of specimens exhibit a reduction in failure stress due to impact damage.

A comparison of failure stresses for the three types of specimens, shown in figure 15, indicates that the graphite-thermoplastic fabric specimens withstand about 12 percent more stress than the graphite-epoxy specimens for impact speeds below about 61 m/sec (impact energy of 5.5 J). Graphite-thermoplastic tape specimens withstand 5 percent more stress than the graphite-epoxy specimens for impact speeds below 61 m/sec. However, the reduction in failure stress due to impact damage is larger in both types of graphite-thermoplastic specimens than in the graphite-epoxy specimens. This difference may be related to the amount of damage sustained when the impact projectile penetrates and passes through the specimens rather than bouncing off the specimens. The impact projectile fully penetrates the graphite-epoxy specimens at impact speeds of more than 73 m/sec (impact energy of 8 J), the fabric specimens at speeds of more than 84 m/sec (impact energy of 10.5 J), and the tape graphite-thermoplastic specimens at speeds of more than 99 m/sec (impact energy of 14.7 J). The filled data points in the figure represent impacts for which the impact projectile penetrated the specimen, and the open data points represent impacts for which the impact projectile bounced off the specimen. C-scans of some specimens after impact indicate that the graphite-epoxy specimens have the smallest damaged area for a given impact energy. In some cases the graphite-thermoplastic tape specimens have damaged areas up to three times as large as the damaged areas of the graphite-epoxy specimens for the same impact energy. The graphite-thermoplastic fabric specimens have damaged areas up to twice as large as the damaged areas of the graphite-epoxy specimens for the same impact energy. The size of the damaged area does not directly correlate to the reduction in failure stress.

Concluding Remarks

An experimental investigation of the compression behavior of laminated specimens made from graphite-epoxy tape (AS4-3502), graphite-thermoplastic tape (AS4-PEEK), and graphite-thermoplastic fabric (AS4-PEEK) was conducted. Specimens with no damage prior to compressive loading, specimens with central circular holes with diameters up to 67 percent of the specimen width, and specimens subjected to low-speed impact damage were loaded to failure in uniaxial compression.

Graphite-thermoplastic tape specimens with holes have up to 15 percent lower failure stresses and strains than graphite-epoxy specimens with the same stacking sequence and hole size. However, graphite-thermoplastic specimens have higher failure stresses and strains than graphite-epoxy specimens of the same stacking sequence and impact energy. Test results for graphite-thermoplastic specimens constructed from unidirectional tape and from fabric indicate that the material form has little effect on failure stresses associated with circular holes or with low-speed impact damage. Compression test results for graphite-thermoplastic specimens with holes or with impact damage and with many clustered plies of the same orientation indicate that having many clustered 0° plies does not influence the static-load-carrying ability of the specimen. The results for the specimens tested indicated that postbuckled graphite-thermoplastic specimens with holes carry

more load than similar postbuckled graphite-epoxy specimens.

NASA Langley Research Center
Hampton, VA 23665-5225
January 17, 1991

References

1. Williams, Jerry G.; O'Brien, T. Kevin; and Chapman, A. J., III: Comparison of Toughened Composite Laminates Using NASA Standard Damage Tolerance Tests. *ACEE Composite Structures Technology—Review of Selected NASA Research on Composite Materials and Structures,* NASA CP-2321, 1984, pp. 51–73.
2. Starnes, J. H., Jr.; Rhodes, M. D.; and Williams, J. G.: Effect of Impact Damage and Holes on the Compressive Strength of a Graphite/Epoxy Laminate. *Nondestructive Evaluation and Flaw Criticality for Composite Materials,* R. B. Pipes, ed., ASTM Spec. Tech. Publ. 696, c.1979, pp. 145–171.
3. Whetstone, W. D.: *EISI-EAL Engineering Analysis Language Reference Manual—EISI-EAL System Level 2091. Volume 1: General Rules and Utility Processors.* Engineering Information Systems, Inc., July 1983.
4. Malik, B.; Palazotto, A.; and Whitney, J.: Notch Strength of GR/PEEK Composite Material at Elevated Temperatures. *Collection of Technical Papers, Part 1—AIAA/ASME/ASCE/AHS 26th Structures, Structural Dynamics and Materials Conference,* Apr. 1985, pp. 203–210. (Available as AIAA-85-0648.)
5. Coquill, Scott L.; and Adams, Donald F.: *Mechanical Properties of Several Neat Polymer Matrix Materials and Unidirectional Carbon Fiber-Reinforced Composites.* NASA CR-181805, 1989.
6. Property Data of Aromatic Polymer Composite, APC-2/Hercules Magnamite® AS4 Carbon Fibre. Data Sheet 3a, ICI-Fiberite.®
7. Rhodes, Marvin D.; Mikulas, Martin M., Jr.; and McGowan, Paul E.: Effects of Orthotropy and Width on the Compression Strength of Graphite-Epoxy Panels With Holes. *AIAA J.,* vol. 22, no. 9, Sept. 1984, pp. 1283–1292.
8. Shuart, Mark J.; and Williams, Jerry G.: Compression Behavior of ±45°-Dominated Laminates With a Circular Hole or Impact Damage. *AIAA J.,* vol. 24, no. 1, Jan. 1986, pp. 115–122.
9. Williams, Jerry G.: *Effect of Impact Damage and Open Holes on the Compression Strength of Tough Resin/High Strain Fiber Laminates.* NASA TM-85756, 1984.
10. Starnes, James H., Jr.; and Rouse, Marshall: Postbuckling and Failure Characteristics of Selected Flat Rectangular Graphite-Epoxy Plates Loaded in Compression. *A Collection of Technical Papers, Part 1—AIAA/ASME/ASCE/AHS 22nd Structures, Structural Dynamics & Materials Conference,* Apr. 1981, pp. 423–434. (Available as AIAA-81-0543.)

Table I. Stacking Sequence and Specimen Designation

Designation*	Stacking sequence	Material	Number of specimens tested
Specimens with 0° plies			
T1	$[(\pm 45)_2/0_4/90/\pm 45/0_2/90]_s$	AS4-PEEK, tape	14
T2	$[(\pm 45)_3/0_2/90/(\pm 45)_2/0/\overline{90}]_s$	AS4-PEEK, tape	14
T3	$[\pm 45/0_6/\pm 45/0_6]_s$	AS4-PEEK, tape	14
T4	$[\pm 45/0_6/\pm 45/0_6/\overline{90}]_s$	AS4-PEEK, tape	14
E1	$[(\pm 45)_2/0_4/90/\pm 45/0_2/90]_s$	AS4-3502, tape	15
E3	$[\pm 45/0_6/\pm 45/0_6]_s$	AS4-3502, tape	8
E4	$[\pm 45/0_6/\pm 45/0_6/\overline{90}]_s$	AS4-3502, tape	8
F2	$[(\pm 45)_3/0_2/90/(\pm 45)_2/0/\overline{90}]_s$	AS4-PEEK, fabric	15
Specimens with no 0° plies			
E5	$[(\pm 45)_2/\overline{90}]_s$	AS4-3502, tape	15
T5	$[(\pm 45)_2/\overline{90}]_s$	AS4-PEEK, tape	15
F5	$[(\pm 45)_2/\overline{90}]_s$	AS4-PEEK, fabric	13

*Letter refers to material and construction type; number refers to stacking sequence.

Table II. Description of $[(\pm 45)_2/0_4/90/\pm 45/0_2/90]_s$ Specimens

Specimen	Cross-sectional area,* A, cm^2	Hole diameter, a, cm	Impact energy, J	Failure stress, MPa	Failure strain
E1-1	2.81	0.00	0	536.4	0.00902
E1-2	2.82	.79	0	418.4	.00681
E1-3	2.83	1.27	0	345.6	.00584
E1-4	2.83	1.91	0	394.3	.00697
E1-5	2.83	2.54	0	316.3	.00563
E1-6	2.84	3.81	0	251.5	.00537
E1-7	2.82	5.08	0	165.4	.00447
E1-8	2.82	0	1.36	578.1	.01080
E1-9	2.81	0	3.17	501.8	.00870
E1-10	2.80	0	3.09	408.9	.00640
E1-11	2.84	0	5.77	293.4	.00490
E1-12	2.84	0	10.6	195.5	.00441
E1-13	2.81	0	15.8	167.0	.00339
E1-14	2.84	0	16.9	183.0	.00395
E1-15	2.80	0	24.9	193.6	.00331
T1-1	2.89	0	0	532.7	.01110
T1-2	2.94	.79	0	379.9	.00666
T1-3	2.90	1.27	0	329.6	.00577
T1-4	2.99	1.91	0	288.5	.00550
T1-5	2.92	2.54	0	240.9	.00451
T1-6	2.92	3.81	0	192.4	.00415
T1-7	2.90	5.08	0	132.0	.00367
T1-8	2.88	0	1.33	526.0	.00990
T1-9	2.88	0	3.09	398.5	.00670
T1-10	2.88	0	5.64	347.8	.00620
T1-11	2.88	0	10.6	314.5	.00567
T1-12	2.89	0	17.9	242.8	.00500
T1-13	2.92	0	24.6	211.8	.00449
T1-14	2.95	0	33.9	202.0	.00440

*Nominal length is 25.4 cm; width is 7.62 cm; thickness is 0.38 cm.

Table III. Description of $[(\pm 45)_3/0_2/90/(\pm 45)_2/0/\overline{90}]_s$, $[\pm 45/0_6/\pm 45/0_6]_s$, $[\pm 45/0_6/\pm 45/0_6/\overline{90}]_s$, and $[(\pm 45)_2/\overline{90}]_s$ Specimens

Specimen designation	Average cross-sectional area,* A, cm^2	Range of hole diameters, a, cm	Range of impact energies, J
T2	2.99	0–5.08	
T2	4.03		0–28.1
F2	2.85	0–5.08	
F2	3.86		0–29.0
T3	3.33	0–5.08	
T3	3.36		0–34.8
T4	3.43	0–5.08	
T4	3.41		0–33.9
E3	3.26	0–5.08	
E3	3.24		0–34.7
E4	3.32	0–5.08	
E4	3.34		0–34.3
E5	.965	0–5.08	
E5	.953		0–22.7
T5	.966	0–5.08	
T5	.939		0–34.8
F5	.886	0–5.08	
F5	.921		0–22.9

*Nominal length is 25.4 cm; width is 7.62 cm in all specimens except impacted T2 and F2. Thickness is 0.38 cm for stacking sequence 2, 0.43 cm for stacking sequences 3 and 4, and 0.127 cm for stacking sequence 5.

Table IV. Material Properties

Material	AS4-3502 graphite-epoxy	AS4-PEEK graphite-thermoplastic
Longitudinal Young's modulus, E_1, GPa . . .	127.6	133.8
Transverse Young's modulus, E_2, GPa	11.3	8.9
Shear modulus, G_{12}, GPa	6.0	5.1
Poisson's ratio, μ_{12}	.3	.38

NASA
National Aeronautics and Space Administration

Report Documentation Page

1. Report No.	2. Government Accession No.	3. Recipient's Catalog No.
NASA TP-3071		

4. Title and Subtitle	5. Report Date
Compression Behavior of Graphite-Thermoplastic and Graphite-Epoxy Panels With Circular Holes or Impact Damage	March 1991
	6. Performing Organization Code
7. Author(s)	8. Performing Organization Report No.
Dawn C. Jegley	L-16853
9. Performing Organization Name and Address	10. Work Unit No.
NASA Langley Research Center Hampton, VA 23665-5225	505-63-01-09
	11. Contract or Grant No.
12. Sponsoring Agency Name and Address	13. Type of Report and Period Covered
National Aeronautics and Space Administration Washington, DC 20546-0001	Technical Paper
	14. Sponsoring Agency Code

15. Supplementary Notes

16. Abstract

An experimental investigation of the compression behavior of laminated specimens made from graphite-epoxy tape, graphite-thermoplastic tape, and graphite-thermoplastic fabric was conducted. Specimens with five different stacking sequences were loaded to failure in uniaxial compression. Some of the specimens had central circular holes with diameters up to 67 percent of the specimen width. Other specimens were subjected to low-speed impact with impact energies up to 35 J prior to compressive loading. This investigation indicates that graphite-thermoplastic specimens with holes have up to 15 percent lower failure stresses and strains than graphite-epoxy specimens with the same stacking sequence and hole size. However, graphite-thermoplastic specimens subjected to low-speed impact have up to 15 percent higher failure stresses and strains than graphite-epoxy specimens with the same stacking sequence and impact energy. Compression tests of graphite-thermoplastic specimens constructed of fabric and unidirectional tape indicate that the material form has little effect on failure strains in specimens with holes or low-speed impact damage.

17. Key Words (Suggested by Authors(s))
Graphite-epoxy
Graphite-thermoplastic
Impact damage
Open hole compression

18. Distribution Statement
Unclassified—Unlimited

Subject Category 24

19. Security Classif. (of this report)	20. Security Classif. (of this page)	21. No. of Pages	22. Price
Unclassified	Unclassified	16	A03